We are IntechOpen,
the world's leading publisher of
Open Access books
Built by scientists, for scientists

6,900
Open access books available

185,000
International authors and editors

200M
Downloads

Our authors are among the

154
Countries delivered to

TOP 1%
most cited scientists

12.2%
Contributors from top 500 universities

CLARIVATE ANALYTICS
BOOK CITATION INDEX
INDEXED

WEB OF SCIENCE™

Selection of our books indexed in the Book Citation Index
in Web of Science™ Core Collection (BKCI)

Interested in publishing with us?
Contact book.department@intechopen.com

Detection and Warning of Tsunamis Generated by Marine Landslides

Mal Heron

Abstract

Seismic signals provide an effective early detection of tsunamis that are generated by earthquakes, and for epicentres in the hard-rock subduction zones there is a robust analysis procedure that uses a global network of seismometers. For earthquakes with epicentres in soft layers in the upper subduction zones the processes are slower and the seismic signals have lower frequencies. For these soft-rock earthquakes a given earthquake magnitude can produce a bigger tsunami amplitude than the same earthquake magnitude in a hard rock rupture. Numerical modelling for the propagation from earthquake-generated tsunamis can predict time of arrivals at distant coastal impact zones. A global network of deep-water pressure sensors is used to detect and confirm tsunamis in the open ocean. Submarine landslide and coastal collapse tsunamis, meteo-tsunamis, and other disturbances with no significant seismicity must rely on the deep-water pressure sensors and HF radar for detection and warning. Local observations by HF radar at key impact sites detect and confirm tsunami time and amplitude in the order of 20–60 minutes before impact. HF radar systems that were developed for mapping the dynamics of coastal currents have demonstrated a capability to detect tsunamis within about 80 km of the coast and where the water depth is less than 200 m. These systems have now been optimised for tsunami detection and some installations are operating continuously to provide real-time data into tsunami warning centres. The value of a system to warn of hazards is realised only when coastal communities are informed and aware of the dangers.

Keywords: tsunami, marine landslides, hazards, warnings, HF radar

1. Introduction

The phenomenon of 'tsunami' occurs very often in large bodies of water around the world. The great majority of these are small, even unnoticeable, but have the physical characteristics of a shallow-water gravity wave with periods 10–40 minutes, which define a tsunami. The recording of tsunamis has historically been based on the amount of damage to coastal communities and the magnitude of a submarine earthquake on the moment magnitude scale (M_w) which has been developed from the Richter Scale [1]. These are effectively logarithmic energy scales. Neither of these metrics relate well to the amplitude of the associated tsunami wave in the open ocean, which is a more reliable metric because a medium-scale earthquake (M_w = 7) in a landslide earthquake can generate the same tsunami amplitude as a severe (M_w = 9) earthquake in a deeper hard-rock subduction zone.

Because of the absence of a standard, the records of 'notable' tsunamis vary among authors, but a general consensus emerges that there is one major tsunami about every 3 years, of which about 75% are caused by earthquakes originating from megathrusts in hard rock. The remaining 25% are mostly landslide tsunamis. The genesis of tsunamis varies with locations and while any large water body like lakes and inland seas are susceptible, it is the so-called ring of fire around the Pacific that has the highest tsunami occurrence of about 80% [2].

Tsunami warning methods fall into three categories. The first arises from the analysis of seismic data collected in the region of the earthquake epicentre. Seismic signals recorded on seismometers located on land near to an earthquake epicentre are used to report estimates of the magnitude and location within a few minutes of the rupture [3]. This can be extended to differentiating between landslide tsunamis and hard-rock megathrust tsunamis [4, 5] by analysing the periodicity in the seismic signals.

The second warning category is obtained through ocean observations in the deep ocean. A network of DART ((Deep-ocean Assessment and Reporting of Tsunamis) moorings consist of a benthic pressure sensor to detect small, but sustained, changes in water depth and a surface buoy for communications [6]. DART moorings can detect tsunamis with amplitudes greater than about 3 cm, and immediately transmit an alert via a satellite link. A network of DART moorings is coupled with seismometers and numerical modelling to warn of potential tsunami impacts around the coastal boundaries of that ocean basin.

The third warning category is at the site of potential impact. Observations of tsunamis approaching in the shallow water on the continental at a critical site give alerts that are accurate in timing and amplitude, but are issued typically less than one hour before impact. The main value of these technologies is to confirm alerts if they have already been given from the epicentre location and the mid-ocean systems, and also to issue warnings for tsunamis generated in the local area. The most promising technology in this category is HF ocean radar that can detect an approaching tsunami at a range of about 100 km, or at the edge of the continental shelf if that is closer than 100 km. The resolution of DART technology and HF radars are consistent with the suggestion that a tsunami wave with an amplitude greater than 0.03 m in the deep ocean should be considered potentially hazardous when it impacts the coast.

Included in this third category of warnings at the site of impact is a cultural awareness of local people to look at the ocean and understand visible changes. For example, any list of 'notable' historic tsunamis recorded would start with a report by Herodotus in 479 BC during the Persian siege of the town of Potidaea (reported by [7]) as "a great flood-tide, higher, as the people of place say, than any one of the many that had been before" which obliterated the Persians who thought they had taken a strategic advantage of the preceding retreat of the water. Herotodus had written the first record of a tsunami impact. Up to half of tsunami impacts on the coast have an initial draw-down which (with suitable education) serves as an excellent warning for local people. Local warnings like HF radar are imperative when the tsunami approaches as a crest.

The well-established global network of seismometers can produce location and magnitude estimates within a few minutes of the event. Based on these data, numerical modelling (e.g. [8]) is used to forecast arrival times of any resulting tsunami at coastal sites around the world using properties of tsunamis which propagate as shallow water gravity waves (even in the deepest oceans!) with a velocity given by
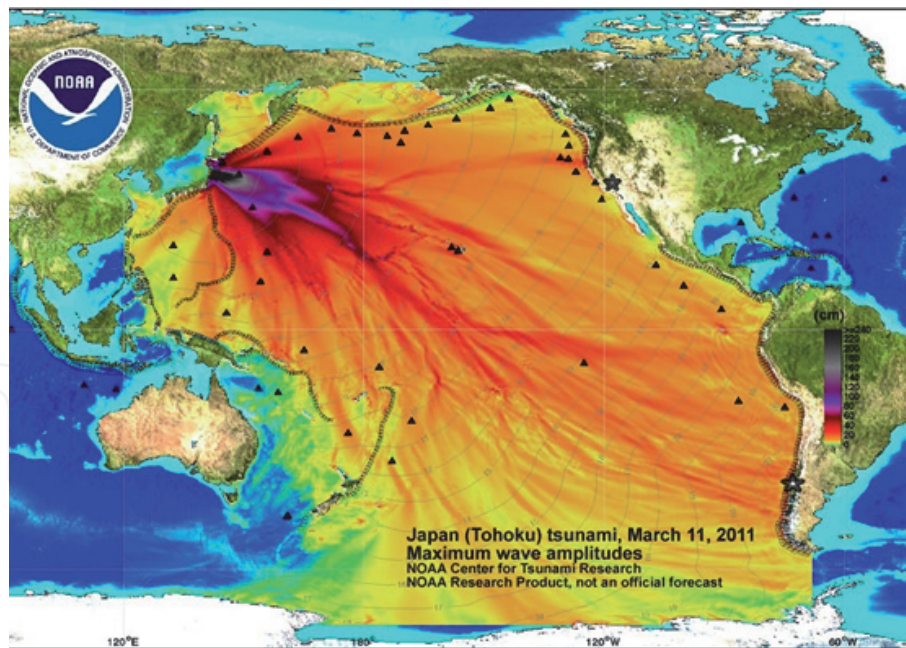
$$c = \sqrt{gh} \qquad\qquad (1)$$

Figure 1.
Maximum tsunami amplitudes calculated by the MOST model for 24 hours following the magnitude 9.0 earthquake near Tohuko, Japan on 11 march 2011. The faint grey contours show the estimated times of arrival. http://nctr.pmel.noaa.gov.

where g is gravitational acceleration and h is the depth of the water column. At $h = 3000$ m the tsunami speed is about 170 ms^{-1} and on a continental shelf of depth 50 m it is about 30 ms^{-1}. This dramatic slowing-down near the coast raises the value of local observations at impact sites.

The propagation characteristics of the Tohuko Earthquake 2011 shown in **Figure 1** are calculated by the MOST (Method of Splitting Tsunami, [8]) model for the Pacific Ocean following the earthquake with epicentre 29 km deep and 130 km from the east coast of Honshu. This computation is a heavy load and, in practice many warning centres have a library of scalable forecasts for tsunamis that are pre-calculated for a range of magnitudes and epicentres at regular spacing (say 100 km) along likely fault zones.

The most critical place for rapid warnings is the adjacent coast which for the Tohuko earthquake, had tsunami impact approximately 84 minutes after the seismic signals. This is a typical warning time in the local region where the tsunami amplitudes are greatest (**Figure 1**). Deep water DART Buoys in the Pacific Ocean can confirm the magnitude of the tsunami, with appropriate delays in the order of hours (**Figure 1**). Arrival of the tsunami at all impact zones can be confirmed by local observations and warnings. In most cases the local confirmation of an imminent tsunami would be issued as a follow-up on prior alerts for the event, but for landslide tsunamis, coastal collapse tsunamis and other non-seismic tsunamis the local observations may be the only way to give the primary warning.

2. Seismic signal warnings

Seismometers provide the traditional data for the estimation of magnitude and location of the epicentre of an earthquake, and a global network of instruments provides rapid and reliable information. The development of seismometry has traditionally been focused on earthquakes from megathrusts of hard rock in the subduction zones, but recent work has been reported on ruptures in shallow, soft

rock subduction zones and submarine landslides which produce seismic signals that have different characteristics.

2.1 Seismic signals from tsunamigenic earthquakes

Data from seismometers in the region of an earthquake have been the traditional means of issuing tsunami warnings. So-called Tsunamigenic Earthquakes result mainly from shearing movement at the tectonic plate boundaries and volcanic hot spots in the lithosphere. Tsunamigenic earthquakes typically occur when there are vertical as well as horizontal components in megathrusts on fault lines in the hard rock deep in subduction zones beneath the ocean floor. The energy given to a resulting tsunami comes from the potential energy released during the seismic thrust. The original Richter Scale for earthquake magnitude is illustrated in **Figure 2** from Richter's book [1] where the maximum amplitude of the P waves, and the delay between S and P signals are used to determine the earthquake magnitude.

The relationship between Richter's magnitude and the rupture is given by Aki [9] as:

$$M = \mu A D \qquad (2)$$

where D is the slip, μ is the rock rigidity, and A is an area equal to $D \times W$, where W is the depth of the fracture.

Richter's method did not take account of the spectrum of components in the seismic signal, and saturates when $M > 8$. Kanamori [10] considered a range of spectral components in the seismic signal to define a Moment Magnitude, M_w, which agrees with Richter's magnitude for small earthquakes, is accurate for $M_w > 9$, and is now widely used to specify earthquake magnitudes (even though it is often
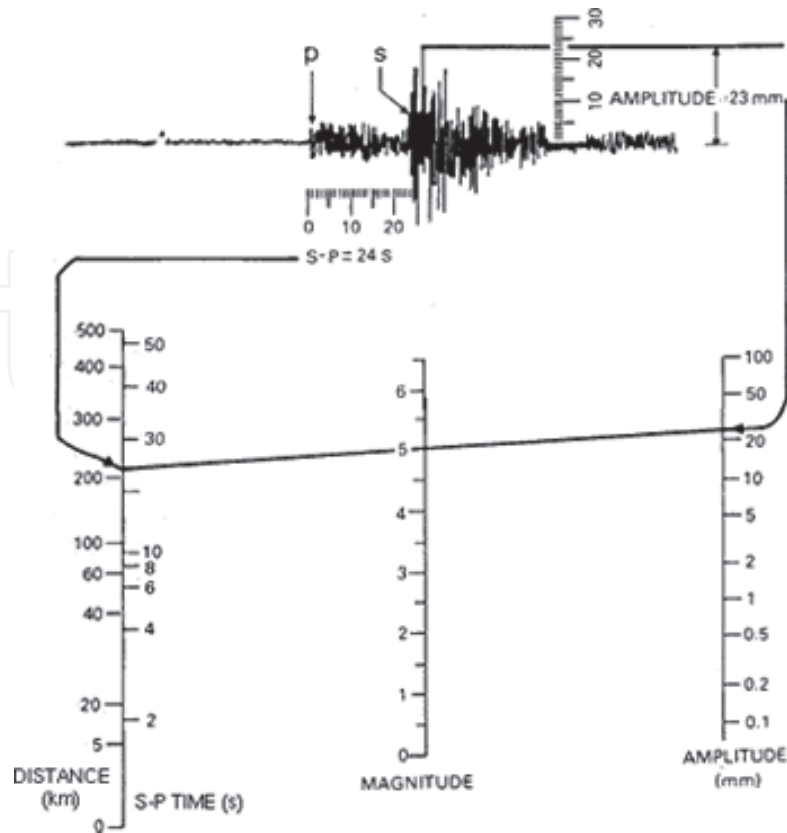

Figure 2.
Richter's relationship between the seismic signals and the logarithmic Richter scale. From Richter, Elementary Seismology [1].

called the Richter Scale). The simplest approach for tsunami warnings is that if M_w > 8.0 and the epicentre is offshore then it is likely that a tsunami will be generated.

Working towards a strategy to provide rapid local tsunami warnings, Melgar et al. [3] use scaling relationships

$$log_{10}D = -2.37 + 0.57M_w \qquad (3)$$

$$log_{10}W = -1.86 + 0.46M_w \qquad (4)$$

to estimate the width and length of an earthquake deformation based on M_w. Then, using the predefined slab model of Hayes et al. [11] they estimate horizontal and vertical deformations of the sea floor, and the magnitude of resulting tsunamis. This strategy provides estimates of tsunami genesis from hard rock ruptures that are sufficiently accurate to provide tsunami warnings. This method is shown to deliver warnings within a few minutes of the rupture and is the basis of warning systems in Japan, Indonesia and Australia [12, 13]. For the 2011 Tohoku earthquake the rapid estimate gave M_w = 9.3 when the final value was calculated at M_w = 9.0. The subsequent propagation of the tsunami is shown in **Figure 1** which is calculated by the MOST model.

2.2 Seismic signals from landslide earthquakes

The name Tsunami Earthquake was coined by Kanamori [14] and does not include the Tsunamigenic Earthquakes discussed in the previous section. These are tsunamis that are significantly bigger than one would predict from the seismic data, and are generated by deformation in the soft rock in the upper subduction layer or by a submarine landslide in a thick, stratified sedimentary layer on a bathymetric slope.

The Mentawai earthquake off the west coast of Sumatra, Indonesia on 25 October 2010 had a medium magnitude of 7.8 but produced a large tsunami that caused significant coastal damage and loss of over 400 lives. This tsunami was significantly greater than would normally be expected from an earthquake of that magnitude. Analysis of the seismic records [4, 5] showed that the Mentawai earthquake was a result of slow deformation in the upper layers of the subduction zone.

Earlier work by Kanamori [14] had shown that weak earthquakes with slow deformation time constants could produce significant tsunamis. This work was done using data from the Aleutian Islands earthquake of 1946, and the Sanriku earthquake of 1896, both of which were relatively weak earthquakes that produced very large tsunamis. Slow deformation, of around 100 s, does not generate high frequency seismic signals like those shown in **Figure 2** and Kanamori's conclusion is that the abnormally slow deformation at the source of the earthquake generated the tsunami. This is consistent with tsunamis from submarine landslides following ruptures in the weakly coupled soft rock layer on the inner margins of ocean trenches.

Sahakian et al. [15] compared the seismic signals from six earthquakes of similar magnitude of 7.6–7.9, which were chosen because GPS data on earthquake amplitudes were available from GNSS recordings, as well as a local seismometer station. The six earthquakes were Ibaraki, Japan 2011; Nicoya, Costa Rica 2012; Iquique, Chile 2014; Melinka, Chile 2016; and Mentawai, Indonesia 2010. In **Figure 3** the acceleration from the local seismometer, and the vertical displacement time series are shown on the same ordinate scale.

From these data, Sahakian et al. [15] confirmed that the Mentawai earthquake in the soft rock in the upper levels of the subduction zone did not generate the
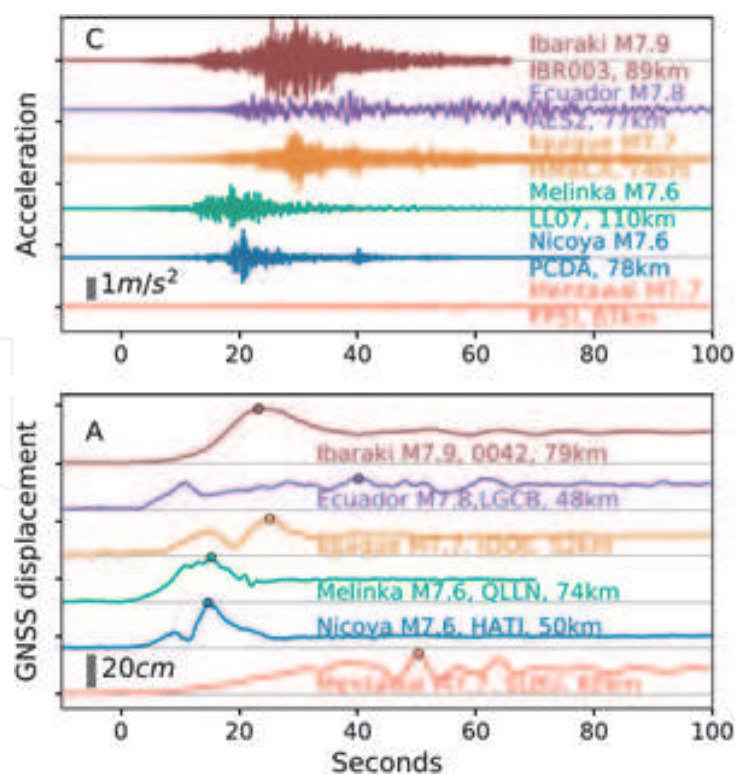
Figure 3.
Data from five earthquakes with similar magnitudes in the 7.6–7.9 range. The earthquake name and magnitude, the seismometer station name and its distance from the epicentre are given for each event. The Mentawi earthquake, and to a lesser extent Ecuador, have smaller accelerations in the seismic signal but comparable vertical displacements in the GNSS data. From Sahakian [15] USGS doi.org/10.3133/circ1187.

high-frequency seismic signals that are generated by megathrusts of earthquakes in the hard rock deeper in the zone. If the slower fluctuations are accompanied by large amplitudes, then it is concluded that the amplitude-to-energy ratio can be used to detect a tsunami earthquake when the magnitude is lower. By comparing fluctuation amplitudes (observed by GPS) with earthquake energy, Sahakian showed that it is possible to issue an alert for a potential tsunami from a tsunamigenic earthquake.

Sahakian et al. [15] suggested a method for early warnings of Tsunami Earthquakes is to estimate M_{PGA} from the seismometer and M_{PGD} from the GNSS vertical displacements. Then a low M_{PGA} coupled with a high M_{PGD} suggests that the event has ruptured soft and compliant rock high in the subduction zone with a high likelihood of producing a large tsunami.

3. Open Ocean observations

Observations in the open and deep ocean are used to give tsunami warnings to locations in the ocean basin that are a long way from the earthquake epicentre. These warnings are relevant to the most severe earthquakes because of the attenuation and geometric spreading of tsunami waves across an ocean basin as shown in **Figure 1** for the 2011 Tohuku earthquake and tsunami.

Even the largest of destructive tsunamis have relatively small amplitudes of up to a few tens of centimetres in deep water. This is illustrated by the altimeter data recorded by the JASON-1 satellite in an opportunistic transit 2 hours after the Sumatra-Andaman earthquake 26 December 2004 [16]. The altimeter recorded a maximum water elevation of about 50 cm in open ocean compared with reports of elevations up to 30 m at some coastal impact points. A DART buoy in the Bay of
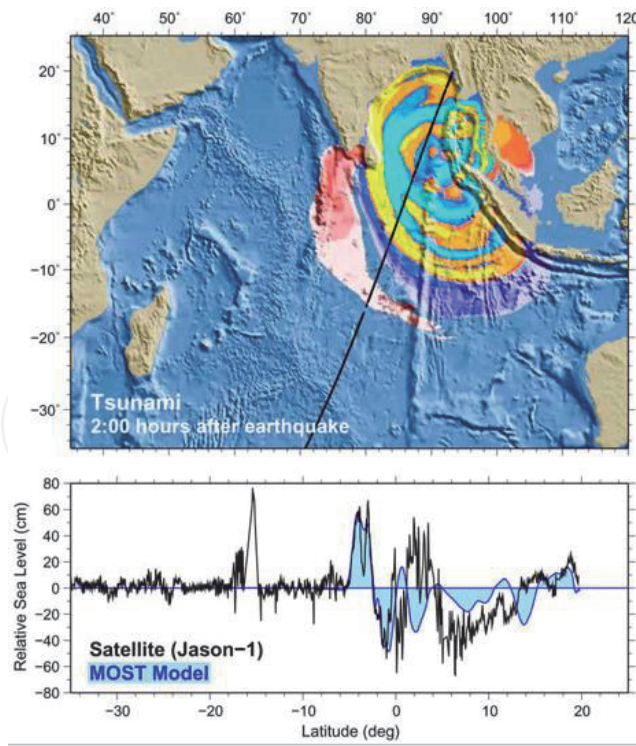
Figure 4.
Transit path of Jason-1 altimeter superposed on estimated elevations from the MOST model 2 hours after the Sumatra-Andaman 2004 earthquake. The maximum water elevation was about 50 cm. From Gower [16] Taylor and Francis tandfonline.com.

Bengal would have given operational confirmation of the timing and warning of the scale of the tsunami.

DART buoys consist of a bottom-mounted pressure sensor with a cable connection to a surface buoy which communicates to a monitoring laboratory through the Iridium network. The pressure sensor takes 15-sec time series at sensitivity of 1 mm of sea water and filters out the high frequencies. If two successive 15-sec averages exceed a projection from the past 3 hours by more than 3 cm the system goes into rapid reporting mode to send data every minute [17, 18]. Following the Sumatra-Andaman earthquake NOAA/PMEL developed an ETD (Easy to Deploy) upgrade to the DART system [19] and this technology is being adopted widely (**Figure 4**) to enable national tsunami warning centres to improve warning systems. The DART system is robust and makes a significant contribution to tsunami warning. DART buoys provide a critical element of the global tsunami warning capability but need to be complemented by seismic and GPS systems for regional warnings near to the epicentre, and systems for warnings in local impact areas whether they are near to the epicentre or distant across oceans.

4. Local impact observations

Apart from visual observations at the beach, the only real-time technology for imminent impacts of tsunamis is land-based HF ocean radar. Observations can only be made over shallow waters <200 m deep in coastal waters, which can give warnings typically 20–60 minutes before impact. To be effective as a warning method HF radar needs to be supported as much as possible with seismic-based alerts or warnings from DART buoys. For tsunamis generated in the local region, especially landslide or coastal collapse events, the local warning from an HF radar may be the only alert possible.

A significant feature not illustrated in **Figure 1** is the growth in amplitude of a tsunami as it slows down in shallow water. As a first-order approximation this growth can be estimated following Green [20] as

$$a(d) = a(D)(D/d)^{1/4} \qquad (5)$$

where a is tsunami amplitude, d is water depth, and D is a reference (deep water) depth. An example of this phenomenon is illustrated by **Figure 5** which shows the amplitude of the Sumatra-Andaman tsunami as about 50 cm in the open water of Bengal Bay, when the tsunami later rose to near 30 m in some impact areas. Associated with the amplification is an enhancement of the velocities of water particles in the propagating wave. The circulating water particles in a gravity wave are manifest on the surface as the to-and-fro motion that can be observed as a swell wave propagates past a point on the ocean. The increase in the maximum to-and-fro velocity, v_m, is [21];

$$v_m(d) = v_m(D)(D/d)^{3/4}. \qquad (6)$$

The primary product of land-based HF ocean radars is surface currents mapped at high spatial resolution over the coastal ocean, and over 400 systems have been installed around the world for that purpose [22]. The potential for HF radars to observe tsunamis was suggested by Barrick [23] and confirmed when several HF radars in Japan as well as North and South America recorded signals as the tsunami from the Tohuko 2011 earthquake reached the west coast of the Americas [24, 25]. In these cases the radars were configured for currents in coastal circulation dynamics, and following the events of March 2011 there was a focus on optimising HF radars for real-time tsunami observations by measuring $v_m(d)$ in Eq. (6).

There are two main HF radar technologies that are widely available for mapping surface currents in coastal waters. Both radar systems operate by receiving radar echoes from the rough, conducting sea surface, and both technologies use timing to define the range of a target zone on the ocean. But they have quite different solutions for determining the angle in the (r,θ) plane. One is the Seasonde system which uses wide angle crossed-loop receiving antennas to define the pointing direction of the radar [23]; and the other is the WERA system which uses a phased
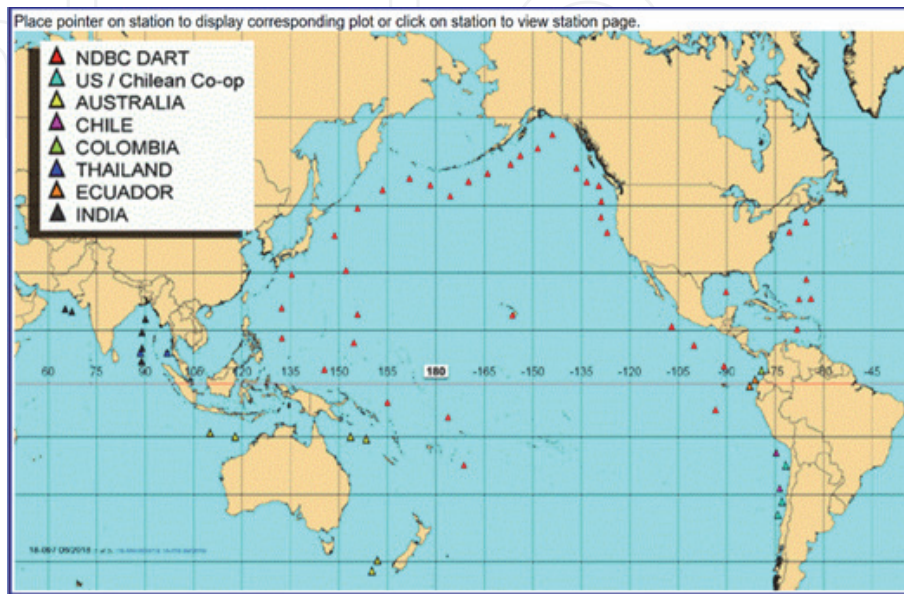

Figure 5.
Global network of DART buoys. www.ndbc.noaa.gov/dart.shtml accessed 21 July 2021.

array of elements as the receive antenna to define azimuth [26]. This differentiation leads to quite different solutions to the challenge of issuing warnings for imminent tsunamis.

The Seasonde software offers a q-factor calculation developed empirically from past tsunami observations and simulations [27, 28]. The observation area is partitioned into strips 2 km wide running parallel to the benthic contours. When the radial current components in three adjacent strips are highly correlated, are showing a trend in magnitude, and are significantly different from the background current, the q-factor index is incremented. **Figure 6** shows the q-factor calculated for data from a Seasonde radar at Point Estero, California (marked with a solid 'x' in **Figure 1**) following the Tohuko 2011 earthquake. Time series of the average current in each strip are taken every 4 minutes, and **Figure 6** shows the data over three strips with the q-factor calculated from the three strips in the 8–14 km range. Tsunami warnings are issued when the q-factor exceeds a trigger level that is set for the conditions prevailing at the specific site, but typically the trigger level is q = 500. Note that the data shown in **Figure 6** were taken from a radar installation optimised for current dynamics, and not for tsunamis. It is a proof of concept.

A WERA station at Rumena in Chile (marked with an 'x' in **Figure 1**) also recorded the tsunami from the Tohuko, 2011 earthquake. In **Figure 7** the colours show current anomaly, with the background removed, with time and range for the beam in the NW direction. From these data and simulations, Gurgel et al. [30] and Dzvonkovskaya et al. [29] developed a probability approach where a time series is
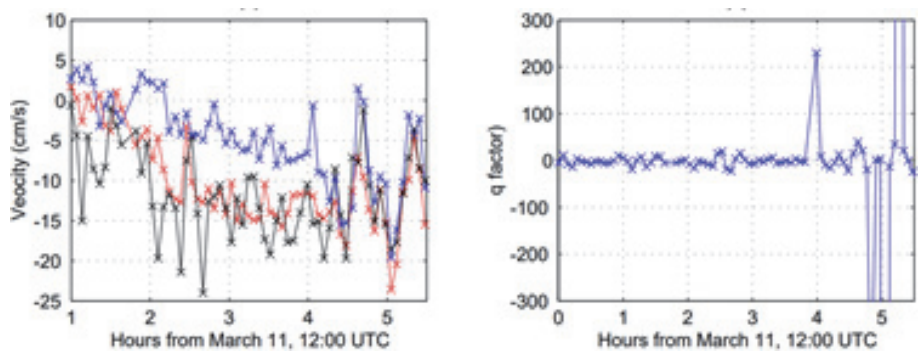

Figure 6.
SeaSonde time series of onshore velocity components and q-factors at point Estero (a) blue: 8–10 km offshore; red: 10–12 km offshore, and black: 12–14 km offshore; (b) q-factor for the 8–14 km interval. From Lipa et al. [25].
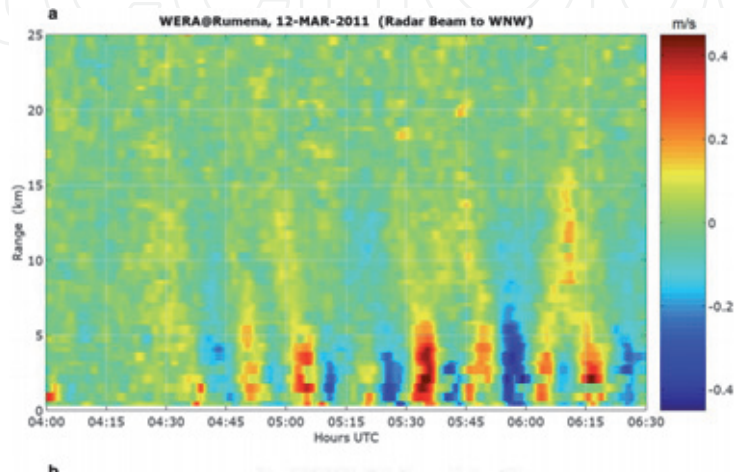

Figure 7.
Surface currents on a time vs. range visualisation for the Tohuko 2011 tsunami approaching the coast at Rumena, Chile. From Dzvonkovskaya et al. [29].

taken over 133 s for each grid point over the mapped area and a probability of an anomalous current (compared with background currents) is assessed at each point. A probability map is produced from 133-second overlapping time series and issued every 33 s. An example of a probability map is shown in **Figure 8** for the data set from the Tohuko 2011 tsunami taken at Rumena at 0545 UT, some 45 minutes before impact. Note that the data shown in **Figures 7** and **8** were taken from a radar installation optimised for current dynamics, and not for tsunamis. It is a proof of concept.

Dzvonkovskaya et al. [29, 31] further developed this method into a robust algorithm for an estimation of the 'Probability of Tsunami' for the site. The final tsunami warning product is produced by statistical processing of successive 2D probability maps. An example of the alerts and warnings issued in real time for a WERA system configured for tsunami warnings is shown in **Figure 9**. This event
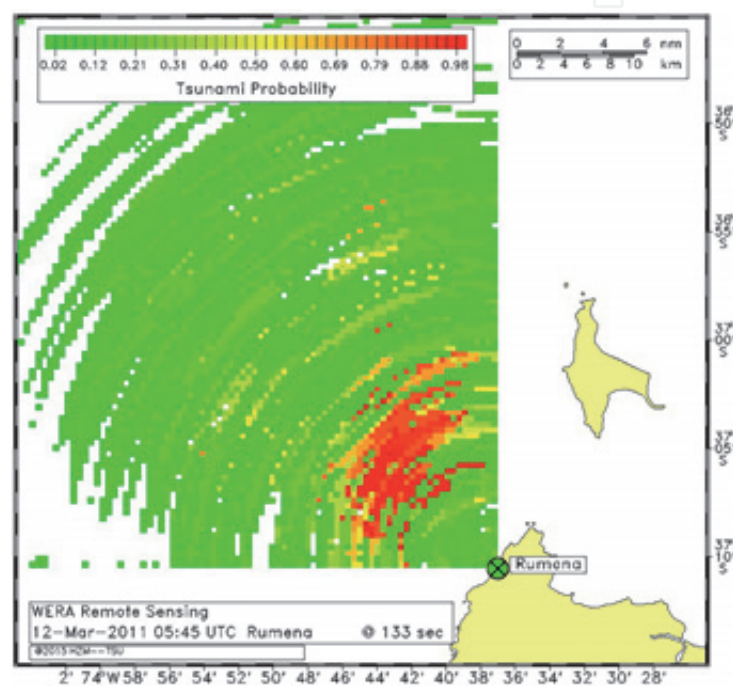

Figure 8.
Map of estimates of tsunami probability for independent grid points from the WERA radar at Rumena following the Tohuko 2011 earthquake. From Dzvonkovskaya et al. [29].
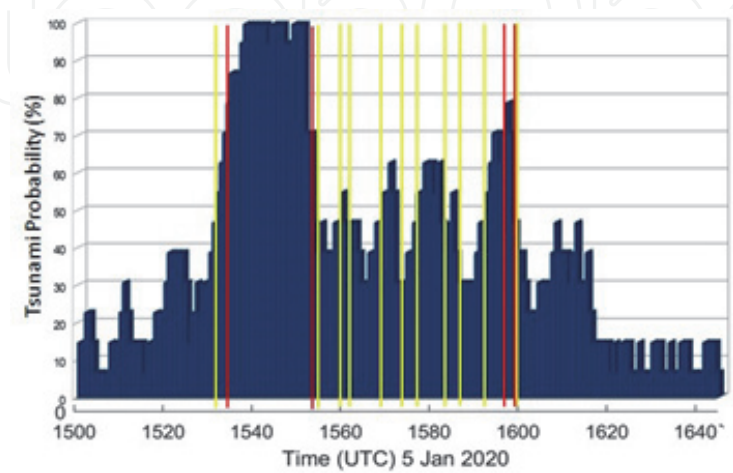

Figure 9.
Tsunami probability for the WERA radar for Tofino, Canada. Surface currents from the whole grid are combined to give a single probability index that is issued every 33 s in real time. 'ATTENTION' is issued when the tsunami probability exceeds 50% (between yellow lines) and 'ALERT' is issued at 75% (between red lines) in real-time.
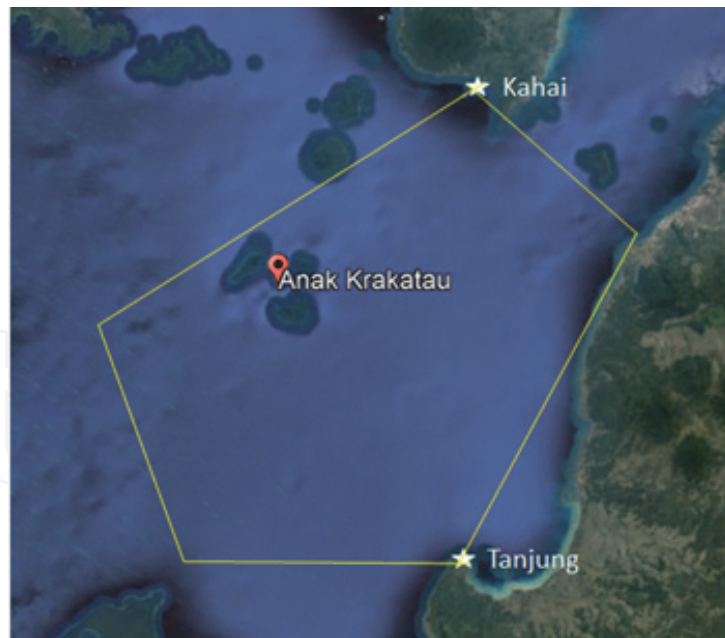
Figure 10.
WERA HF radar stations at Tanjung and Kahai deployed for detecting tsunamis in the irregular pentagon inside the yellow lines. This is a part of the GITEWS for warning of tsunamis generated in the Krakatoa caldera. Base image GoogleEarth.

was a tsunami-like disturbance produced by a severe meteorological front at Tofino, British Columbia, Canada in 2020. The Tsunami Probability (TP) bulletins are issued every 33 seconds to the host system. The recommended warning levels are issued as 'attention' if $50 < TP < 75$, and as 'alert' if $TP > 75$ as shown in **Figure 9** for the event at Tofino.

HF radars have been deployed at several places with the primary purpose of tsunami warning where data are returned in real time to a tsunami warning centre. One of these is in the Sunda Strait where the volcano island Anak Krakatau appeared above the sea in 1927 on the edge of the Krakatoa Caldera formed in 1883. After several days of seismic activity in December 2018, it erupted with an area of about 64 hectares and volume of 0.2 km^3 collapsing into the sea generating a tsunami that resulted in 437 fatalities and over 30,000 injuries on the adjacent Java and Sumatra islands [32]. The collapse had no strong short-period seismic signals and did not provide a seismic tsunami warning. In view of the volcanic activity in the area, the German Indonesian Tsunami Early Warning System (GITEWS) was established as an integrated system for warning of locally generated tsunamis with sensors including seismic, acoustic and HF radar [33]. The configuration of the HF radar stations is shown in **Figure 10**. This radar installation is being used primarily in the GITEWS system but is also producing maps of surface currents over the area outlined by the irregular pentagon in **Figure 10**. There is a strong interest in the ocean dynamics in the Sunda Strait because the long-term flow-through of warm water from the Java Sea to the Indian Ocean is a key driver of ocean circulation. This WERA system produces current maps on a 1×1 km grid every 20 minutes for circulation applications, and evaluate tsunami activity every 33 s on a continuous schedule.

5. Conclusion

Tsunamis generated by hard-rock megathrust earthquakes, like Tohuko 2011 in the Pacific and Sumatra-Andaman 2004 in the Indian Ocean, give high-frequency

seismic signals from which reliable, fast estimates of tsunami amplitudes are produced, and propagation modelling across neighbouring oceans can be made, with reliable confirmation from deep-ocean DART buoys. For these tsunamis, confirmation at key coastal sites is useful because shallow-water bathymetry and coastal topography are significant parameters for the terrestrial run-up of water. The warning systems for tsunamis generated by hard-rock megathrust earthquakes are robust and are widely used. Routine monitoring is being used at coastal sites that have infrastructure or populations at risk. The use of HF radar at key at-risk sites gives final confirmation of amplitude and timing before tsunami impact.

Tsunamigenic soft-rock earthquakes in the upper subduction zone have slow-response seismic signals that can lead to underestimation of resulting tsunamis if hard-rock algorithms are used. There is active development of methodology to estimate the amplitudes of tsunamis from tsunamigenic earthquakes using regional seismic and GPS signals. Data from the Mentawai 2010 earthquake and tsunami have provided a foundation for the development of this method. Implementation requires installation of GPS (GNSS) monitoring of earthquake amplitudes in regions where there are known unstable sedimentary bedforms. Tsunamis from tsunamigenic earthquakes are detected on DART buoys and local monitoring at key at-risk sites on the coast gives confirmation. Local monitoring may be the primary warning at impact sites close to the epicentre.

Submarine landslides and coastal collapse have produced damaging tsunamis with impacts mostly confined to the local region. These tsunamis have no seismic warnings. Other tsunami genesis mechanisms without seismicity include glacial calving, which is localised, and meteotsunamis which are generated by meteorological fronts and similar in scale to storm surges at the coast. The seismic and DART technologies are less applicable to these events because most damage has been in the source region and local monitoring takes on more urgency. HF radar is a proven technology for tsunami detection in shallow coastal waters where warnings can be issued in the order of 20–60 minutes before impact (depending on the width of the shallow coastal shelf). While HF radars have been installed primarily for tsunami detection and warning in several regions, they can also provide maps of coastal currents for research and management of coastal industries like ports, marine reserves and coastal engineering. There are over 400 HF radar installations worldwide [22], usually in regions of high economic or social interest. A useful strategy in the short term would be to retro-fit existing HF radars that have tsunami detection capability, with tsunami detection software that is integrated into central tsunami warning hubs.

Acknowledgements

Author details

Mal Heron
Marine Geophysics Laboratory and Physical Sciences, James Cook University,
Australia

*Address all correspondence to: mal.heron@ieee.org

IntechOpen

References

[1] Richter, C.F., Elementary Seismology, 768 pp., 205 illus. W. H. Freeman and Company, San Francisco, and Bailey Bros. and Swinfen Ltd., 75 London, 1958. www.US.macmillan.com

[2] National Geographic Society. Tsunamis. National Geographic. Accessed March 1, 2014. http://environment.nationalgeographic.com/environment/natural-disasters/tsunami-profile/.

[3] Melgar, D., Allen, R. M., Riquelme, S., Geng, J., Bravo, F., Baez, J. C., et al. (2016). Local tsunami warnings: Perspectives from recent large events. Geophysical Research Letters, 43, 1109–1117. DOI:10.1002/2015GL067100

[4] Lay, T., C.J. Ammon, H. Kanamori, Y. Yamazaki, K.F. Cheung and A.R. Hutko, The 25 October 2020 Mentawai tsunami earthquake (Mw 7.8) and tsunami hazard presented by shallow megathrust ruptures, Geophys. Res. Letters, 38, 5pp, L06302, 2011. DOI: 10.1029/2010GL046552.

[5] Newman, A.V., G. Hayes, Y. Wei and J. Convers, The 25 October 2010 Mentawai tsunami earthquake, from real-time discriminants, finite-fault rupture, and tsunami excitation, Geophys. Res. Letters, 38, L05302, 2011. DOI:10.1029/2010GL046498.

[6] Bernard, E., and C. Meinig (2011): History and future of deep-ocean tsunami measurements. In Proceedings of Oceans' 11 MTS/IEEE, Kona, IEEE, Piscataway, NJ, 19–22 September 2011, 15 No. 6106894, 7 pp.

[7] Smid, T. C. 'Tsunamis' in Greek Literature. Greece and Rome, 2nd Ser., Vol. 17, No. 1 (April 1970), pp. 100–04 (102f.)

[8] Titov, V. V., F. I. Gonzalez, E. N. Bernard, M. C. Eble and H. O. Mofjeld, Real-time tsunami forecasting: Challenges and solutions, in Developing Tsunami-resilient Communities, ed E. N. Bernard, pp. 41-58, Springer, Netherlands, 2005

[9] Aki, K., Earthquake Mechanism, Tectonophysics, 13, 423-446, 1972 do: 10.1016/0040-1951(72)90032-7

[10] Kanamori, H. The energy release in great earthquakes, J. Geophys. Res., 82 (20): 2981–2987, 1977. doi:10.1029/jb082i020p02981.

[11] Hayes, G. P., D. L. Wald, and R. L. Johnson (2012), Slab1.0: A three-dimensional model of global subduction zone geometries, J. Geophys. Res., 117, B01302, DOI:10.1029/2011JB008524.

[12] Allen, S. C. R., and D. J. M. Greenslade (2008), Developing tsunami warnings from numerical model output, Nat. Hazards, 46(1), 35–52. 06

[13] Hoshiba, M., and T. Ozaki, Earthquake early warning and tsunami warning of the Japan Meteorological Agency, and their performance in the 2011 off the Pacific Coast of Tohoku Earthquake (M_w 9.0), in Early Warning for Geological Disasters, eds F. Wenzel and J. Zschau, pp. 1-28, Springer, Berlin, 2014.

[14] Kanamori, H. (1972). Mechanism of 82 tsunami earthquakes. Physics of the 83 Earth and Planetary Interiors. 6 (5): 84 346–359. DOI:10.1016/0031-9201 (72) 85 90058-1

[15] Sahakian, V. J., Melgar, D., and Muzli, M., Weak near-field behavior of a tsunami earthquake: Toward real-time identification for local warning. Geophys. Res. Letters, 46, 2019. DOI: 86 10.1029/2019GL083989

[16] Gower, J. (2007). The 26 December 2004 tsunami measured by satellite

altimetry, Int. J. Remote Sens., 28, 2897–2913, DOI:10.1080/01431160601094484. Taylor and Francis www.tandfonline.com.

[17] Meinig, C., S.E. Stalin, A.I. Nakamura, F. González, and H.G. Milburn (2005): Technology Developments in Real-Time Tsunami Measuring, Monitoring and Forecasting. In Oceans 2005 MTS/IEEE, 19–23 September 2005, Washington.

[18] Milburn, H.B., A.I. Nakamura and F.I. Gonzalez, Real-Time Tsunami Reporting from the Deep Ocean, Proc. MTS/IEEE OCEANS, September 1991.

[19] Lawson, R.A., D. Graham, S. Stalin, C. Meinig, D. Tagawa, N. Lawrence-Slavas, R. Hibbins, and B. Ingham (2011): From Research to Commercial Operations: The Next Generation Easy-to-Deploy (ETD) Tsunami Assessment Buoy. In Proceedings of Oceans'11 MTS/IEEE, Kona, IEEE, Piscataway, NJ, 19–22 September 2011, No. 6107114, 8 pp

[20] Green G, On the Motion of Waves in a Canal of Variable Depth G Green - Cam. Phil. Trans., VI: 1837. 457 p.

[21] Kinsman, B., Wind Waves, Prentice-Hall, Englewood Cliffs, NJ, USA, 1965.

[22] Roarty H, Cook T, Hazard L, George D, Harlan J, Cosoli S, et al., 2019. The Global High Frequency Radar Network. Front. Mar. Sci. 6:164. DOI: 10.3389/fmars.2019.00164

[23] Barrick, D., A coastal radar system for tsunami warning, Rem. Sens. Env., 8, 353-358, 1979 DOI:10.1016/0034-4257(79)90034-8

[24] Dzvonkovskaya, A., Ocean surface current measurements using HF radar during the 2011 Japan tsunami hitting Chilean coast. In: Proc. of IEEE IGARSS20 2012, Munich, Germany, 2012, pp. 7605-7608, DOI:10.1109/IGARSS.2012.6351867.

[25] Lipa, B., J. Isaacson, B. Nyden and D. Barrick, Tsunami arrival detection with high frequency (HF) radar, Remote Sens. 2012, 4(5), 1448-1461; DOI:10.3390/rs4051448

[26] Gurgel KW, Antonischki G, Essen HH, et al. Wellen radar (WERA): A new ground-wave HF radar for ocean remote sensing. Coastal Engineering. 1999;37: 219–234.

[27] Lipa, B., D. Barrick and J. Isaacson, Coastal tsunami warning with deployed HF radar systems, Chapter 5 in Tsunami, Mohammad Moktari (Ed.), InTech. 2016. DOI:10.5772/63960. Available Online: http://www.intechopen.com/books/tsunami/coastal-tsunami-warning-with-deployed-HF-radar-systems

[28] Lipa, B., H. Parikh, D. Barrick, H. Roarty, and S. Glenn. High frequency radar observations of the June 2013 US East Coast Meteotsunami, Nat Hazards (2014) 74:109–122 DOI 10.1007/s11069-013-0992-4.

[29] Dzvonkovskaya, A., L. Petersen, T. Helzel, and M. Kniephoff, High Frequency Ocean radar support for tsunami early warning systems, Geosci. Res. Letters, 5:29, 2018. DOI:10.1186/s40562-018-0128-5.

[30] Gurgel K-W, Dzvonkovskaya A, Pohlmann T, Schlick T, Gill E (2011) Simulation and detection of tsunami signatures in ocean surface currents measured by HF radar. Ocean Dynamics, Springer. DOI:10.1007/s10236-011-0420-9

[31] Dzvonkovskaya, A., 2018. HF surface wave radar for tsunami alerting: From system concept and simulations to integration into early warning systems, IEEE A&ES Mag 33:48–58. DOI: 34 10.1109/MAES.2018.160267

[32] Ye, L., H. Kanamori, L. Rivera, T. Lay, Y. Zhou, D. Sianipar and K. Satake, The 22 December 2018 Tsunami from Flank Collapse of Anak Krakatau Volcano during Eruption, Science Advances, 6/3, eaaz1377, 2020. DOI: 10.1126/sciadv.aaz1377

[33] Gomez, R., T. H. Tran, A. Ramdhani, and R. Triyono, HF Radar Validation and Accuracy Analysis using Baseline Comparison Approach in the Sunda Strait. Global Oceans 2020: Singapore – U.S. Gulf Coast, 2020, pp. 1-5, DOI: 10.1109/IEEECONF38699.2020.9389158